Fluid Dynamics & Materials Processing
DOI:10.32604/fdmp.2020.07981
Article

Convection-Diffusion Model for Radon Migration in a Three-Dimensional Confined Space in Turbulent Conditions

Shengyang Feng[1,2,3,*], Dongbo Xiong[4], Guojie Chen[5], Yu Cui[1] and Puxin Chen[1]

[1]School of Resource Environment and Safety Engineering, University of South China, Hengyang, 421001, China
[2]Hunan Province Engineering Technology Research Center of Uranium Tailings Treatment, Hengyang, 421001, China
[3]Hunan Province Engineering Research Center of Radioactive Control Technology in Uranium Mining and Metallurgy, Hengyang, 421001, China
[4]Shanghai Institute of Applied Physics, Chinese Academy of Sciences, Shanghai, 201800, China
[5]School of Civil Engineering, University of South China, Hengyang, 421001, China
*Corresponding Author: Shengyang Feng. Email: 14100044@usc.edu.cn
Received: 17 July 2019; Accepted: 14 March 2020

Abstract: Convection and diffusion are the main factors affecting radon migration. In this paper, a coupled diffusion-convection radon migration model is presented taking into account turbulence effects. In particular, the migration of radon is simulated in the framework of the k-ε turbulence model. The model equations are solved in a complex 3D domain by the finite element method (FEM). Special attention is paid to the case study about radon migration in an abandoned air defense shelter (AADS). The results show that air convection in a confined space has a great influence on the radon migration and the radon concentration is inversely proportional to the wind speed.

Keywords: Convective diffusion; radon migration; turbulence; numerical simulation

Abbreviations

C	Radon concentration distribution (Bq/m^3)
D	Diffusion coefficient of radon in the air (1.05×10^{-5} m^2/s)
U	Velocity (m/s)
λ	Decay constant of radon (2.1×10^{-6}/s)
F	Radon source term (Bq/m^3/s)
ρ	Density (kg/m^3)
μ_t	Turbulence viscosity (Pa·s)
Δt	Time difference between the two-point measurement time (h)
k	Turbulent kinetic
ε	Turbulence dissipation rate
P_k	Turbulen ε_t kinetic (k) due to the average velocity gradient
E	Radon exhalation rate (Bq/m^3/s)
C_1,C_2	Concentration of radon at two adjacent moments (Bq/m^3)
A	Opening area of radon-collecting hood (m^2)

λ_V Ventilation rate (h^{-1})
A_{vent} Ventilation area (m^2)

1 Introduction

Pollutants in the confined space are more likely to accumulate, causing harm to people health [1,2]. Radon and its daughters are special among these pollutants because of their radioactivity causing lung cancer [3–5]. Exposure to radon gas and its daughters has long been recognized as a potential health hazard, and long-term inhalation of high radon concentrations may cause lung cancer [6]. Therefore, knowledge of the radon migration in the confined space is of great significance for predicting radon concentration, which provides guides for reducing the harm of radon. In previous studies, common methods are one-dimensional or two-dimensional analytical solution methods [7,8]. However, these methods are not applicable to the three-dimensional case with complex boundary conditions.

At present, there are a few researches on this issue. Rabi et al. [9] simulated the radon concentration distribution in an experimental model room by FORTRAN software. However, the model is relatively simple, only considering the distribution of radon in laminar flow. Collignan et al. [10] and Akbari et al. [11] simulated the indoor radon migration based on convective-diffusion without considering the effect of radon decay term. When the radon migrates in the confined space with high air velocity or complex geometric structure, the turbulence flow must be considered for the numerical model [12,13]. In this paper, we established a three-dimensional model of radon migration in confined space with consideration of turbulence flow and radon diffusion-convection process. A case study of radon migration in an AADS was numerically analyzed by the model.

2 Mathematical Model

2.1 Radon Migration Model

The main theory of radon migration is mainly a combination of the diffusion and convection flow of radon gas [14–16]. The radon migrating in the confined space can be simulated using the following equation [10,15]:

$$\frac{\partial C}{\partial t} = D\Delta C - \nabla(UC) - \lambda C + F \tag{1}$$

where C is the radon concentration distribution (Bq/m^3), D is the diffusion coefficient of radon in the air (1.05×10^{-5} m^2/s), U is the velocity (m/s), λ is the decay constant of radon (2.1×10^{-6}/s), F is radon source term ($Bq/m^3/s$).

Assuming that radon source term in the air is equal to 0, the steady-state radon migration model in confined space may be expressed as:

$$D\Delta C - \nabla(UC) - \lambda C = 0 \tag{2}$$

The key to numerically solving Eq. (2) is to determine the second term, $\nabla(UC)$ which represents the radon convective velocity is closely related to the distribution of the radon concentration in space, and they are coupled with each other. Because air flow in the confined space is highly susceptible to the turbulent flow, it is necessary to use the turbulence model to obtain the convective velocity in the confined space, so as to establish a coupling relationship between the convective velocity and radon diffusion.

2.2 Air Turbulence Model in Confined Space

In this paper, the air turbulent flow is simulated using the k-ε turbulence model. The k-ε turbulence model is a two-equation model to simulate the air turbulent flow. The model includes two parameters: k (turbulent

kinetic) and ε (turbulence dissipation rate) [17,18]. In general, the air turbulent flow in the confined space is assumed to be small and incompressible so that it can be simulated by solving two variables (velocity and length scale).

Turbulence viscosity (μ_t) is expressed by the turbulent kinetic, k, and turbulence dissipation rate, ε, as:

$$\mu_t = \rho C_\mu \frac{k^2}{\varepsilon} \tag{3}$$

where ρ is density (m/s), μ_t is turbulence viscosity (Pa·s), $C_\mu = 0.19$ [19]. In the case of incompressible steady flow, the transport equation of turbulent kinetic, k, and turbulence dissipation rate, ε, can be reduced to:

$$\rho(u \cdot \nabla)k = \nabla \cdot \left[\left(\mu + \frac{\mu_t}{\sigma_k}\right)\nabla k\right] + P_k - \rho\varepsilon \tag{4}$$

$$\rho(u \cdot \nabla)\varepsilon = \nabla \cdot \left[\left(\mu + \frac{\mu_t}{\sigma_k}\right)\nabla \varepsilon\right] + C_{1\varepsilon}P_k\frac{\varepsilon}{k} - C_{2\varepsilon}\rho\frac{\varepsilon^2}{k} \tag{5}$$

where $C_{1\varepsilon} = 1.44$, $C_{2\varepsilon} = 1.92$, $\sigma_k = 1.0$, $\sigma_\varepsilon = 1.3$. P_k is the turbulent kinetic (k) due to the average velocity gradient, expressed as [20]:

$$P_k = \mu_t\left[\nabla u : \left(\nabla u + (\nabla u)^t - \frac{2}{3}(\nabla u)^2\right] - \frac{2}{3}\rho k \nabla \cdot u \tag{6}$$

2.3 Numerical Approach

The FEM is used to numerically calculate the steady-state radon migration model and air turbulence model in the confined space. The FEM is an efficient numerical calculation method, which includes three processes: mesh, element analysis and solving approximate variational equations [21]. In the FEM, the weak form of the three-dimensional steady-state radon migration model is expressed as:

$$\int_\Omega [D\Delta C - \nabla(UC) - \lambda C]\delta C d\Omega = 0 \tag{7}$$

where Ω is the integration domain, in this paper, the whole confined space.

If the radon exhalation rate (the Neumann boundary) is used as a boundary condition, according to the Green formula, Eq. (7) is rewritten as [22]:

$$\int_\Omega [D\Delta C - \nabla(UC) - \lambda C]\delta C d\Omega - \int_\Gamma g\delta C d\Gamma = 0 \tag{8}$$

where g is the radon exhalation rate, and Γ is the boundary of the radon exhalation. Eq. (8) is the weak form of the radon migration model in three-dimensional space.

It is generally believed that free tetrahedral mesh element (FTME) is a good choice for three-dimensional FEM, and its interpolation function can be expressed as:

$$C(x, y, z) = ax + by + cz + d \tag{9}$$

where a, b, c and d are constants. Assuming that the values of the four vertices of the FTME are C_1, C_2, C_3 and C_4, respectively, so:

$$ax_1 + by_1 + czx_1 + d = Cx_1 \tag{10}$$

$$ax_2 + by_2 + czx_2 + d = Cx_2 \tag{11}$$

$$ax_3 + by_3 + czx_3 + d = Cx_3 \tag{12}$$

$$ax_4 + by_4 + czx_4 + d = Cx_4 \tag{13}$$

From Eqs. (9) and (10), it can be obtained as:

$$C(x, y, z) = N_1(x, y, z)C_1 + N_2(x, y, z)C_2 + N_3(x, y, z)C_3 + N_4(x, y, z)C_4 \tag{14}$$

where N_1(x, y, z), N_2(x, y, z), N_3(x, y, z), N_2(x, y, z) are vertex coordinate functions. Eq. (14) can be expressed as a matrix form,

$$C = [N][\delta] \tag{15}$$

where $[N] = [N_1, N_2, N_3, N_4]$, $[\delta] = [C_1, C_2, C_3, C_4]$. Such matrix forms facilitate programming and computer-aided computing. Firstly, the element stiffness matrix is used to integrate the Eq. (8) on the grid element. Secondly, the whole model is calculated by using the balance principle. Thirdly, use constraints to solve linear equations.

The conventional CFD method was applied to numerical calculation of gas turbulence model, which is not discussed in this paper. Schematic diagram of the model proposed in this paper can be seen in Fig. 1. First, the CFD method is used to calculate the convective velocity of the confined space, which is substituted into the steady-state radon migration model. Then, the partial differential equation of the steady-state radon migration model is numerically calculated to obtain the distribution of radon concentrations in the confined space by finite element method.

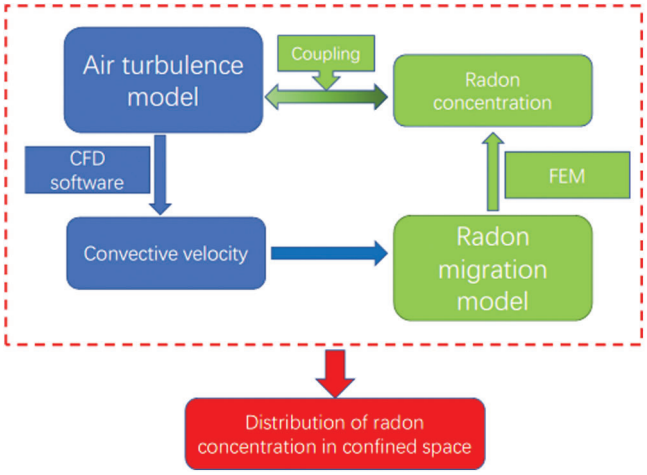

Figure 1: Schematic diagram of formation of the model

2.4 Model Validation

In this research, a room of dimensions 3.01 m × 3.01 m × 3 m (Fig. 2) reported by Chauhan et al. [23] was used to validate the present model. The room has three doors of dimensions 0.9 m × 1.99 m, in which the door No.1 is considered as inlet with velocity of 0.03 m/s, and other two doors (Nos. 2 and 3) are considered as outlet. Radon exhalation rates of walls, floor and ceiling are 1.59 ± 0.1 Bq/m^2/h, 0.96 ± 0.07 Bq/m^2/h

and 0.99 ± 0.19 Bq/m^2/h, respectively. Contours of radon concentration at the height of 1.22 m from the floor is shown in Fig. 3, and the related results proposed by the literature are shown in Fig. 4. Noted that the model for numerical calculation in the literature is time-dependent (transient model), while our model is a steady-state model for predicting radon concentration for an infinitely long time mathematically. This difference determines that calculation results in this paper are larger than those in the literature, and it is not difficult to find from Fig. 4 that the calculated radon concentration in the literature gradually approaches the results in this paper with the increase of time. The verification shows that the method proposed in this paper is effective and reliable.

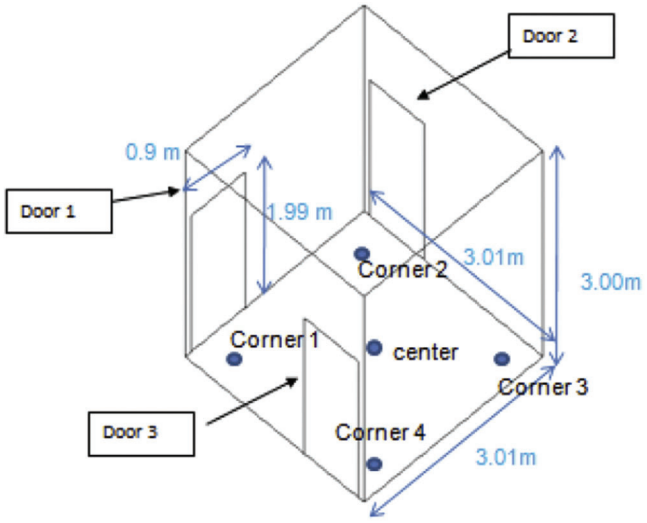

Figure 2: Room geometry

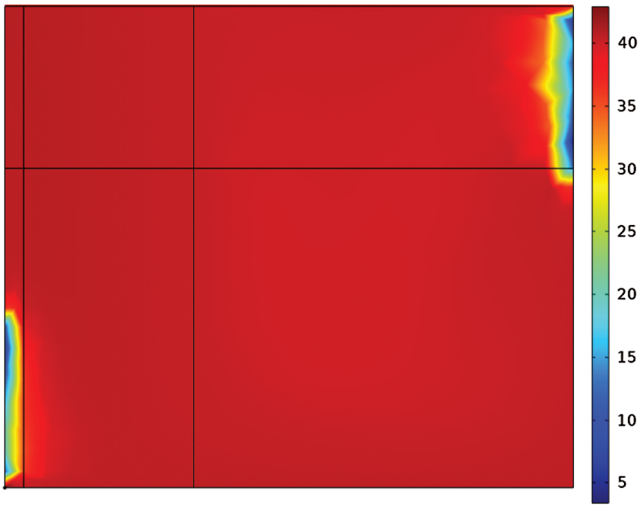

Figure 3: Radon concentration at z = 1.22 m calculated by the presented model (Bq/m^3)

3 Case Study

AADS is a typical confined space with high radon concentration, which is potentially harmful to people health. In this section, we use the aforementioned model to analyze radon migration in an AADS. The AADS

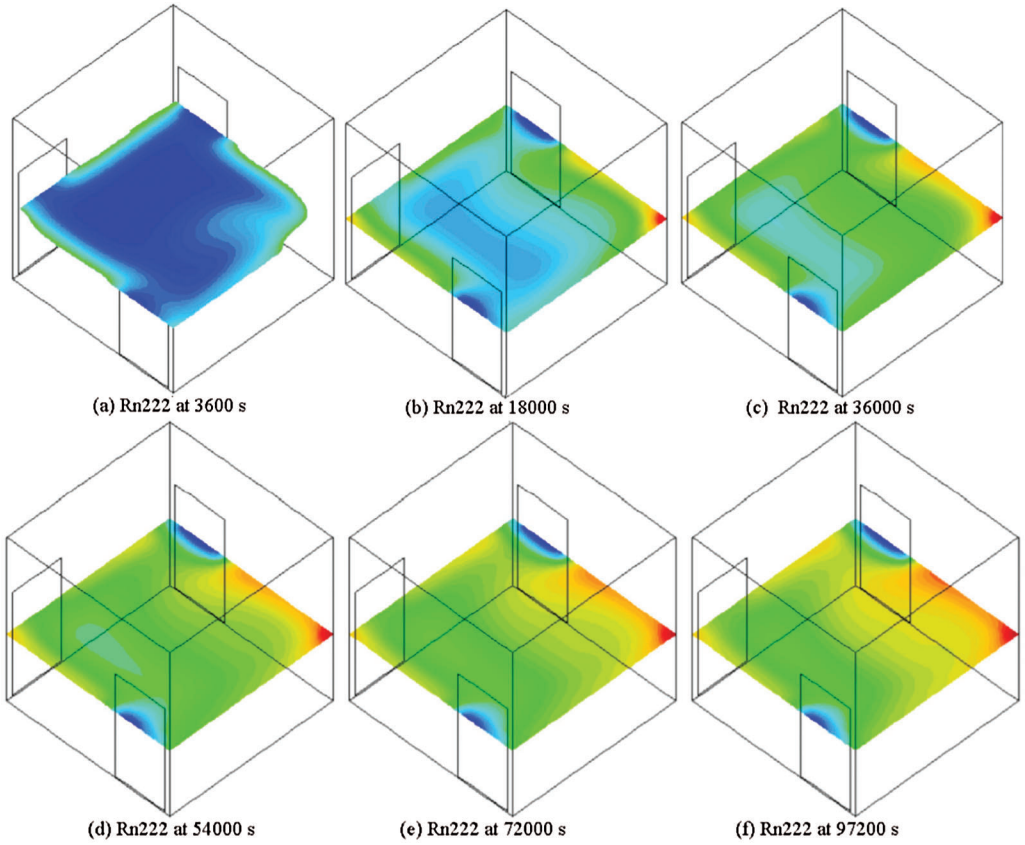

Figure 4: Radon concentration at z = 1.22 m [23] (Bq/m^3)

consists of four laneways and a storage room, as shown in Fig. 5. The width and height of the four lanes are 2 m, the height of the straight wall is 1 m, the radius of the dome is 1 m, and the sectional area of the lane is about 3.57 m^2. The length of No. 1 lane is 12 m, connecting the storage room. The lengths of Nos. 2 and 3 laneway are 13 m, and the No. 4 laneway is 10 m long. The length, width and height of the storage room are 10 m, 8 m and 2 m, respectively. The mesh refinement study has been conducted to find the best optimal mesh parameters for the model of the AADS, which includes 6 boundary-layer elements with the height of the first boundary-layer element of 0.002 m, 633214 domain elements with the maximum size of 0.2 m, and 1695 edge elements with the maximum size of 0.15 m, as shown in Fig. 5.

The initial radon concentration is determined by the radon exhalation rate of the surfaces of the 4 lanes and storage room in the AADS. The radon exhalation rate is measured by the local static method, as shown in Fig. 6. The local static method measures the radon exhalation rate by the increase of radon concentration in unit time by a sealed container [24]. The radon exhalation rate can be obtained by

$$E = \frac{C_2 - C_1}{A \cdot \Delta t} V \tag{16}$$

where E is the radon exhalation rate (Bq/m^3·s), C_1 and C_2 are radon concentrations at two times (Bq/m^3), A is the area of the radon exhalation (m^2), Δt is the time difference between two times (h), V is the volume of radon-collecting hood (m^3). The radon exhalation rates of the AADS are listed in Tab. 1.

The inlet velocity can be calculated by the ventilation rate. The ventilation rate of the shelter is 10 h^{-1} under the condition of natural ventilation. Suppose the AADS has one inlet surface, the amount of inlet air is

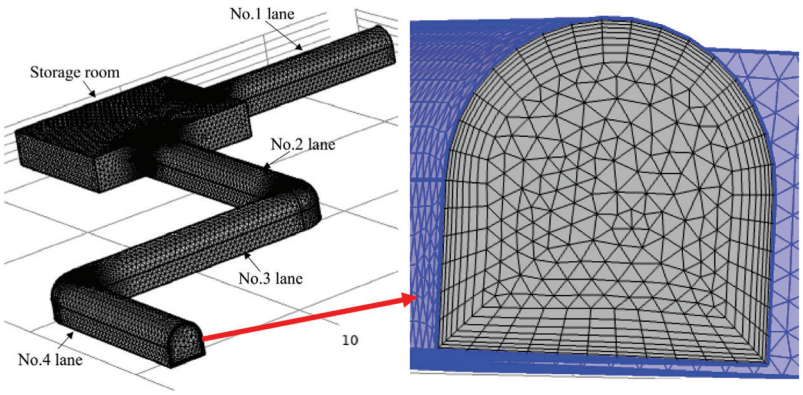

Figure 5: Model meshing

Figure 6: Measurement of radon exhalation rate by local static method

equal to that of outlet air and there is no air flow from the lining, ground and walls in the AADS, the velocity of the inlet boundary is expressed as [9]:

$$U = \frac{{}_V V_{cave}}{A_{vent}} \tag{17}$$

where λ_V is the ventilation rate (h^{-1}), A_{vent} is the ventilation area (3.57 m^2), V_{cave} is the volume of the AADS (338.50 m^3). The pressure of the outlet boundary is 0 Pa.

4 Results and Discussion

Figs. 7 and 8 present numerical calculation results of wind speed and radon concentration of the AADS at z = 1 m. The entrance wind speed of the No. 1 lane is small, and the distribution is more uniform, showing the state of the laminar flow. The radon concentration of the No. 1 lane is also uniformly distributed. In the storage room, due to the complex geometry, the air flow in the storage room is in a turbulent state. The higher concentration of radon from the No. 1 lane follows the air flow into the No. 2 lane, forming a bend-shaped migration path in the storage room, while the radon concentration in the other areas of the storage room is small. Due to the rapid change of the geometry of the air flow channel, the air flow of the No. 2 lane is changed from a relatively smooth layer to a turbulence distribution. The wind speed at the inside of the corner is small, while the outside is large. The distribution of radon concentration is basically consistent with that of the wind speed in the AADS, which means that radon migration in confined space is greatly affected by air convection.

Table 1: Radon exhalation rate in the AADS

Measuring point	Radon exhalation rate ($\times 10^{-4}$ Bq/m^2·s)
Lane 1 ground	1.515
Lane 1 left lining	1.115
Lane 1 right lining	1.310
Lane 2 ground	1.605
Lane 2 left lining	1.025
Lane 2 Right Lining	1.155
Lane 3 ground	1.225
Lane 3 left lining	0.815
Lane 3 Right Lining	0.725
Lane 4 ground	1.260
Lane 4 left lining	1.585
Lane 4 Right Lining	1.190
Top lining of Lane 1	1.213
Top lining of Lane 2	1.090
Top lining of Lane 3	0.770
Top lining of Lane 4	1.125
Ground	1.158
Wall 1	1.160
Wall 2	1.055
Wall 3	1.110
Wall 4	0.915
Ceiling	1.060

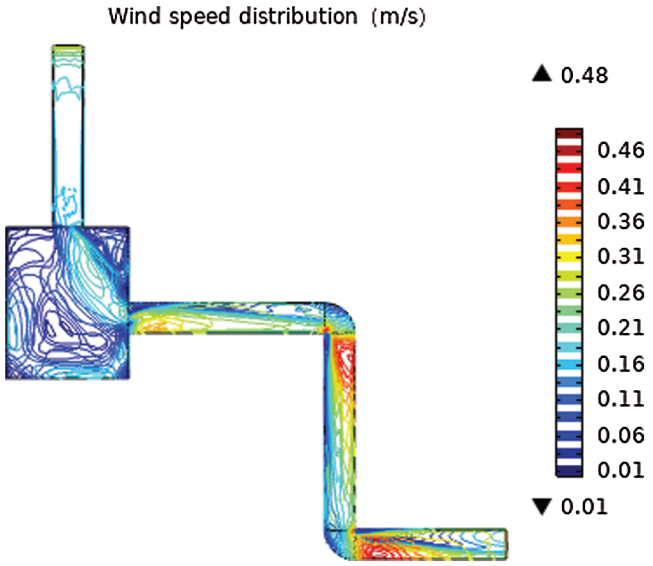

Figure 7: Wind speed distribution at z = 1 m

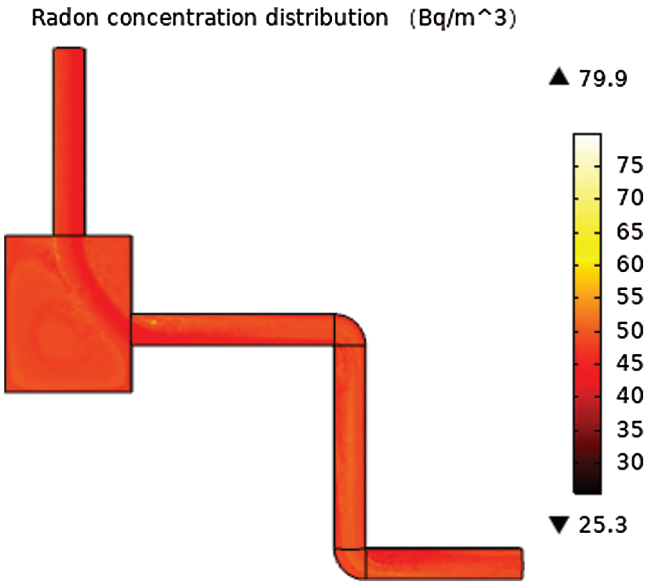

Figure 8: Radon concentration distribution at z = 1 m

Figs. 9 and 10 present wind speed and radon concentration in cross section of the No. 1 and No. 2 lane, respectively. Because the radon exhalation rate of each surface of the AADS is not the same, the radon concentration of the No. 1 lane, where the air flow is in a laminar state, shows a clear layer phenomenon, and the radon concentration is higher near the surfaces with higher radon exhalation rate. In the No. 2 lane, where the air flow is in a turbulent state, the radon concentration is affected by the turbulence flow and inversely proportional to the wind speed. Although the radon exhalation rate of the left lining in No. 2 lane is higher than that of the right lining, the radon concentration in the left lining is lower than that in the right lining because of air convection in confined space.

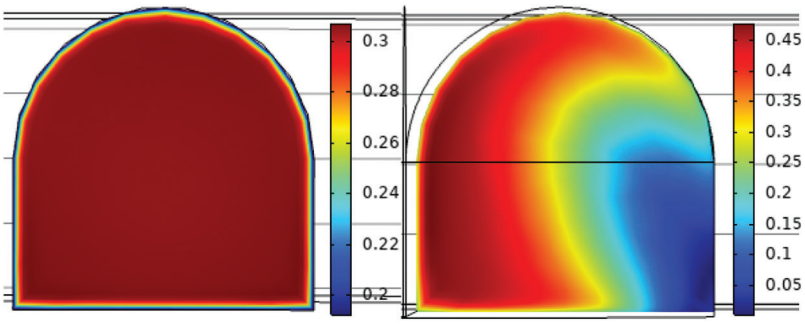

Figure 9: Wind speed in cross section of the No. 1 and No. 2 lane

Fig. 11 shows radon concentration along the central axis of the No. 4 lane, which is consistent with the measured results of He et al. [25]. The radon concentration at the entrance of the confined space is the highest and the minimum at about 1/5 of the longitudinal length, that is close to 2.18 m. The reason is that the diffusion length of radon, defined as the distance it diffuses during its mean lifetime, is 2.18 m in air. Beyond this distance, the radon diffusing from the entrance is neglected, therefore, the radon concentration is the lowest at 2.18 m away from the entrance.

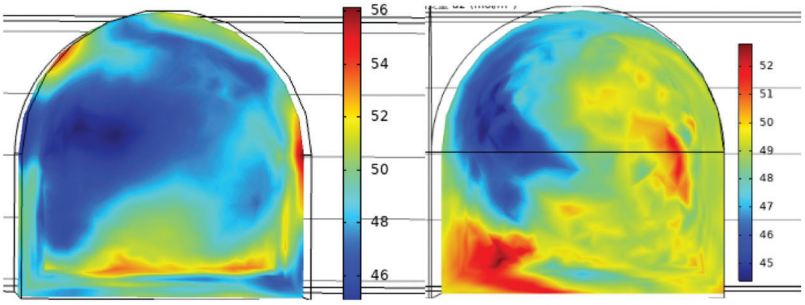

Figure 10: Radon concentration in cross section of the No. 1 and No. 2 lane

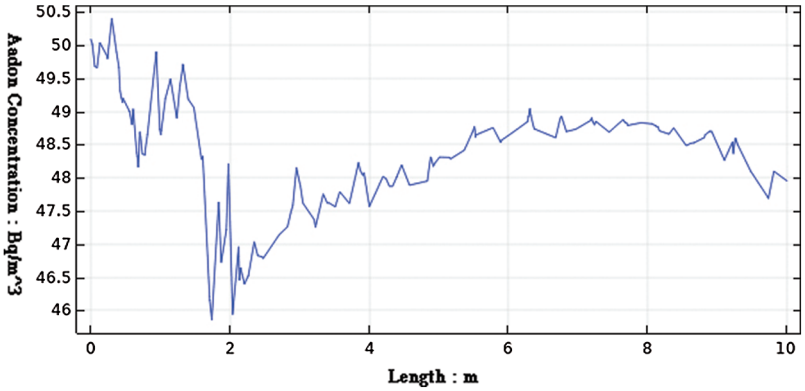

Figure 11: Distribution of radon concentrations along the central axis of the No. 4 lane

We simulated the removal of the diffusion term, $D\Delta C$, or convective term, $\nabla(UC)$, in the radon migration model, Eq. (3). From Fig. 12, it can be seen that if the diffusion term is removed from the radon migration model, the numerical results of the radon concentration will be inconclusive, that is because the velocity of the wall in the k-ε turbulence model is 0, when the radon exhalation rate is taken as the boundary condition, exhalation radon cannot participate in convective action. From Fig. 13, if the convection term is removed

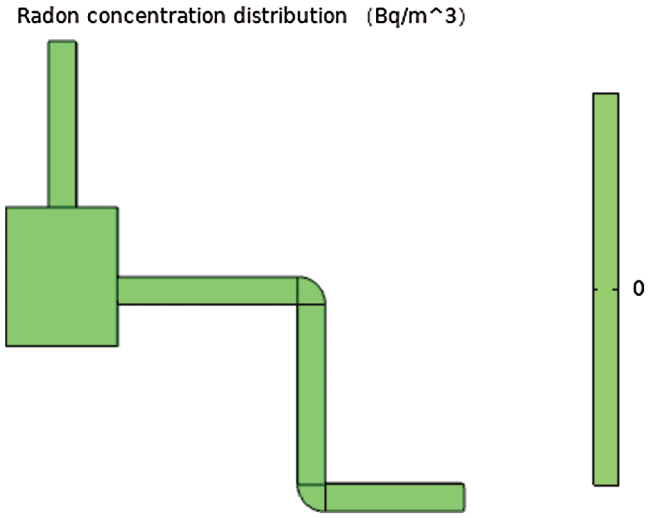

Figure 12: Distribution of radon concentration regardless of diffusion

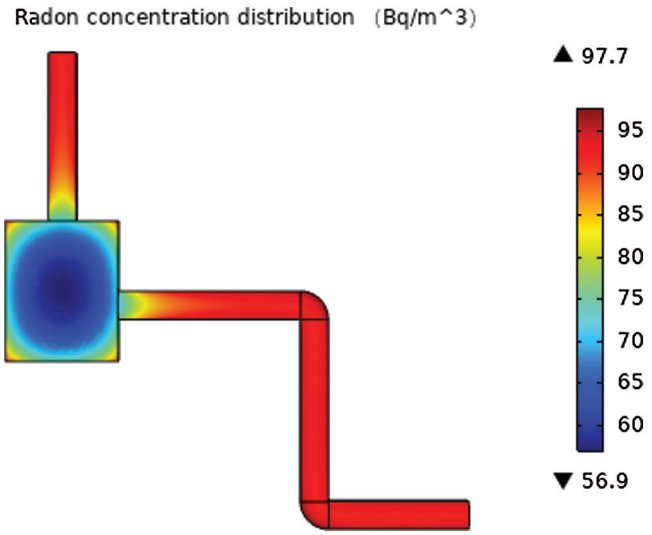

Figure 13: Distribution of radon concentration regardless of convection

from the radon migration model, the radon concentration in the confined space shows a significant gradient change from the precipitated center because of the radon migration only depending on the diffusion of the concentration gradient.

5 Conclusions

In this paper, a three-dimensional model is proposed to study radon migration in confined space and numerically calculated by the FEM. In the model, radon convection migration is simulated by the k-ε turbulence model, while the Fick law is used for radon diffusion migration, and the two are coupled to reflect the interaction between air convection and diffusion during radon migration. The validation study shows that the proposed model is effective and reliable. The model was used to analyze radon migration in an AADS, which is a typical confined space. Results revealed that radon migration in confined space is greatly affected by air convection, and the radon concentration is affected by the turbulence flow and inversely proportional to the wind speed. The radon concentration at the entrance of the confined space is the highest and the minimum at about 2.18 m away from the entrance. By comparing with the simulation results of removing diffusion and convection term from the model, when the radon exhalation rate is taken as the boundary condition, it will cause the calculation results to deviate greatly, affecting the calculation accuracy.

Acknowledgement: The authors would like to thank the Supercomputing Center of University of South China.

Funding Statement: This work was supported by the National Natural Science Foundation of China [grant numbers 11705083], China Postdoctoral Science Foundation [grant number 2018M632975], National Natural Science Foundation of Hunan Province [grant number 2019JJ50488] and Hunan Province Engineering Research Center of Radioactive Control Technology in Uranium Mining and Metallurgy & Hunan Province Engineering Technology Research Center of Uranium Tailings Treatment Technology, University of South China [grant number 2019YKZX1009].

Conflicts of Interest: The authors declare that they have no conflicts of interest to report regarding the present study.

References

1. Dutta, T., Kim, K. H., Minori, U., Pawan, K., Subhasish, D. et al. (2016). The micro-environmental impact of volatile organic compound emissions from large-scale assemblies of people in a confined space. *Environmental Research, 151,* 304–312. DOI 10.1016/j.envres.2016.08.009.
2. Guan, J., Gao, K., Chao, W., Yang, X. D., Chao, H. L. et al. (2014). Measurements of volatile organic compounds in aircraft cabins. Part I: methodology and detected VOC species in 107 commercial flights. *Building and Environment, 72,* 154–161. DOI 10.1016/j.buildenv.2013.11.002.
3. Falkenbach, A., Kleinschmidt, J., Soto, J., Just, G. (2002). Radon progeny activity on skin and hair after speleotherapeutic radon exposure. *Journal of Environmental Radioactivity, 62(3),* 217–223. DOI 10.1016/S0265-931X(01)00164-3.
4. Nancy, V. H., Schwartz, G. G. (2018). Radon and lung cancer: what does the public really know? *Journal of Environmental Radioactivity, 192,* 26–31. DOI 10.1016/j.jenvrad.2018.05.017.
5. Anand, G., Deepak, P. (2018). Inhalation dose due to Rn-222, Rn-220 and their progeny in indoor environments. *Applied Radiation and Isotopes, 132,* 116–121. DOI 10.1016/j.apradiso.2017.11.027.
6. Yoon, J., Lee, J., Joo, S., Kang, D. (2016). Indoor radon exposure and lung cancer: a review of ecological studies. *Occupational and Environmental Medicine, 28(1),* 1–9.
7. Wu, J., Zhang, H., Sun, H. (2014). Numerical simulation for migration rule of fault gas radon in different overburden. *Acta Seismologica Sinica, 36(1),* 118–128.
8. Liu, J., Wang, Z., Wang, X. (2008). The numerical simulation and inversion fitting of radon concentration distribution in homogeneous overburden above active fault zones. *Applied Geophysics, 5(3),* 238–244. DOI 10.1007/s11770-008-0034-2.
9. Rabi, R., Oufni, L. (2018). A theoretical and experimental investigation of spatial distribution of radon in a typical ventilated room. *MAPAN-Journal of Metrology Society of India, 33(2),* 123–130.
10. Collignan, B., Powaga, E. (2017). Impact of ventilation systems and energy savings in a building on the mechanisms governing the indoor radon activity concentration. *Journal of Environmental Radioactivity, 196,* 268–273. DOI 10.1016/j.jenvrad.2017.11.023.
11. Akbari, K., Mahmoudi, J., Ghanbari, M. (2013). Influence of indoor air condition on radon concentration in a detached house. *Journal of Environmental Radioactivity, 116,* 166–173. DOI 10.1016/j.jenvrad.2012.08.013.
12. Han, Y., Chen, D., Liu, S., Xu, G. (2020). An investigation into the effects of the Reynolds number on high-speed trains using a low temperature wind tunnel test facility. *Fluid Dynamics & Materials Processing, 16(1),* 1–19. DOI 10.32604/fdmp.2020.06525.
13. Redchyts, D. O., Shkvar, E. A., Moiseienko, S. V. (2020). Computational simulation of turbulent flow around tractor-trailers. *Fluid Dynamics & Materials Processing, 16(1),* 91–103. DOI 10.32604/fdmp.2020.07933.
14. Karstens, U., Schwingshackl, C., Schmithüsen, D., Levin, I. (2015). A process-based 222radon flux map for Europe and its comparison to long-term observations. *Atmospheric Chemistry & Physics, 15,* 17397–17448.
15. Rogers, V., Nielson, K. (1991). Correlations for predicting air permeabilities and 222Rn diffusion coefficients of soils. *Health Physics, 61(2),* 225–230. DOI 10.1097/00004032-199108000-00006.
16. Feng, S., Wang, H., Cui, Y., Ye, Y., Li, X. et al. (2019). Monte Carlo method for determining radon diffusion coefficients in porous media. *Radiation Measurements, 126,* 1–6. DOI 10.1016/j.radmeas.2019.106130.
17. Wilcox, D. C. (2006). *Turbulence modeling for CFD*. Lake Arrowhead: DCW Industries Inc.
18. Launder, B., Spalding, D. (1972). *Lectures in mathematical models of turbulence*. London: Academic Press.
19. Zhang, Z., Zhang, W., Zhai, Z., Chen, Q. Y. (2007). Evaluation of various turbulence models in predicting airflow and turbulence in enclosed environments by CFD: part 2-comparison with experimental data from literature. *HVAC&R Research, 13(6),* 871–886. DOI 10.1080/10789669.2007.10391460.
20. Zhang, Z., Zhang, W., Zhai, Z., Chen, Q. Y. (2007). Evaluation of various turbulence models in predicting airflow and turbulence in enclosed environments by CFD: part 1-summary of prevalent turbulence models. *HVAC&R Research, 13(6),* 853–870. DOI 10.1080/10789669.2007.10391459.

21. Wrobel, L. C. (1992). Numerical solution of partial differential equations by the finite element method. *Engineering Analysis with Boundary Elements, 9(1),* 106–112. DOI 10.1016/0955-7997(92)90133-R.
22. Claes, J. (1988). *Numerical solutions of partial differential equations by the finite element method*. Cambridge: Cambridge University Press.
23. Chauhan, N., Chauhan, R. P., Joshi, M., Agarwal, T. K., Aggarwal, P. et al. (2014). Study of indoor radon distribution using measurements and CFD modeling. *Journal of Environmental Radioactivity, 136,* 105–111. DOI 10.1016/j.jenvrad.2014.05.020.
24. Stranden, E., Kolstad, A., Lind, B. (1984). The influence of moisture and temperature on radon exhalation. *Radiation Protection Dosimetry, 7(1),* 55–58. DOI 10.1093/rpd/7.1-4.55.
25. He, L., Du, F., Xiong, B., He, L. (2008). Survey of radon concentration in tunnel construction sites and suggestions for protection. *Chinese Journal of Radiological Health, 17(4),* 452–453.